

# Cohoe Radio Observatory, Alaska ~ Part 4, Callisto Antenna System

Whitham D. Reeve

## 1. Introduction

This series of articles describes construction of a new radio observatory in Cohoe, Alaska (see **section 10** for location description). The current part, Part 4, describes a Sun tracking, dual log periodic dipole antenna system that will be used with the new Callisto station at CRO (the e-Callisto solar radio spectrometer network is described at [{e-Callisto}](#)). This will be the first of several antenna systems at the station. Part 4 was delayed while I waited for spring and warmer weather for outdoor mechanical testing of the antenna system. The previous three parts in this series are

- ⚙ Part 1, Radio Frequency Interference Survey [Reeve1]
- ⚙ Part 2, Guyed Tower Foundation Construction [Reeve2]
- ⚙ Part 3, Guyed Tower Installation [Reeve3]

**Note:** Links in braces { } and references in brackets [ ] are provided in **section 12**.

## 2. Antenna System Design Considerations

The antenna system design has both electrical and mechanical considerations. Electrical is straight-forward: First, I initially plan to have the capability to observe solar radio bursts in Callisto's full frequency range 45 to 870 MHz (to be extended later to 17 MHz with an up-converter). Second, because solar radio bursts are partially polarized, the antenna system will be setup to discriminate between right-hand and left-hand circular polarizations. Antenna systems setup to respond to circular polarized emissions also respond to randomly polarized (also called unpolarized) and linearly polarized emissions. For an introduction to radio wave polarization, see [{ReevePol}](#).

To meet the requirements for frequency range, I chose to use two different antenna systems, one based on log periodic antennas for the range from 100 to 870 MHz (Callisto-High) and another based on the Long Wavelength Array (LWA) antenna for the range from 17 to 100 MHz (Callisto-Low). This part describes only the log periodic antenna system used for Callisto-High; a future article will cover the LWA antenna system.

For Callisto-High I will use two commercial log periodic antennas arranged in a crossed configuration (the dipole elements of one antenna are perpendicular to the elements of the other antenna). This arrangement is a compromise; a preferable configuration uses a single antenna structure with crossed-polarized log periodic antennas on a common axis. However, I already had the two antennas, and they are not amenable to modification into a single crossed-polarized antenna. Nevertheless, I am still considering a single purpose-built cross-polarized log periodic antenna for future use.

To increase system sensitivity I will use the TMA-2 tower-mounted amplifier (the TMA-2 is a TMA-1 equipped with two low noise preamplifiers, see [{TMA}](#)). A quadrature coupler will be used to derive circular polarization from the two linearly polarized antennas. For additional information on application of quadrature couplers and antenna systems, see [{ReeveQC}](#).

The mechanical considerations are slightly more involved. I require daily Sun tracking over a wide azimuth and elevation range that varies with the season. During mid-summer the maximum azimuth and elevation ranges are about 300° and 53°, respectively, and during mid-winter the minimum ranges are about 70° azimuth and 6° elevation. To meet the requirement for daily operation, I chose a commercial rotator that uses pulse counting for direction/position sensing rather than a potentiometer, the latter having a limited life as I found in a previous installation. Winter storms can be a problem from a structural perspective so the antenna supports and rotator need to be sturdy. Since requirements change over time and I am always experimenting with antennas, I need to have some flexibility in the antenna support system. In summary, the design resulted in the following major components (figure 1), each to be described in more detail in the following sections:

- 3 ~ Antenna system
- 4 ~ Antenna support structure
- 5 ~ Azimuth/elevation rotator including associated control cables, tower-mounted junction box and mast
- 6 ~ Rotator system setup and tests
- 7 ~ Tower-mounted amplifier assembly
- 8 ~ Transmission line system



Figure 1 ~ Pile of parts: Callisto-High antenna system components fabricated and ready for assembly and testing. Components include dual horizontal support booms (on saw horses), two log periodic antennas (pointed left and right on top of support booms), rotator (black object at right) and tower extensions and top plate (on left) that raise the tower height about 6 ft above the 60 ft height described in Part 3 [Reeve3]. The transmission lines, control cables, tower-mounted amplifier and junction box enclosures are not shown. (Image © 2014, W. Reeve)

### 3. Antenna System

The normal configuration for dipole antennas, and by extension log periodic antennas, setup to receive circular polarizations is to build the two antennas on a common axis with the dipole elements of one antenna perpendicular to the other. However, modifying the two antennas I had on-hand would be very difficult and time consuming. Therefore, I chose to horizontally separate the two antennas and mount them at the ends of a support boom described in the next section. The antenna axes must be perpendicular to the wave front to best discriminate circular polarizations and this is accomplished by tracking the Sun.

Callisto-High uses two identical Creative Design CLP5130-2N log periodic dipole arrays (figure 2). These antennas have 17 elements and a frequency range of 105 to 1300 MHz. Based on a numerical electromagnetic code (NEC) model I prepared for the CLP5130-2N, the free-space gain is about 7 dBi (the peak gain when installed within several wavelengths of the ground is about 12 dBi). One antenna will be tilted laterally  $+45^\circ$  and the other  $-45^\circ$  from horizontal (figure 3). The + and - angles are referenced to the antenna connector at the front of each antenna. When connected through a quadrature coupler, this perpendicular arrangement allows discrimination of right-hand and left-hand circular polarizations. The  $45^\circ$  tilt reduces the effects of ground reflections (thanks to Dick Flagg for that suggestion).



Figure 2 ~ The Creative Design CLP5130-2N log periodic antenna setup for horizontal polarization on a test mast. The antenna is 1.4 m long and the longest element is 1.45 m. The rear boom mount is called a “dragon-fly” mount and adds 0.5 m to the antenna length. The type N RF connector is at the front of the antenna and points down. (Image © 2014, W. Reeve)

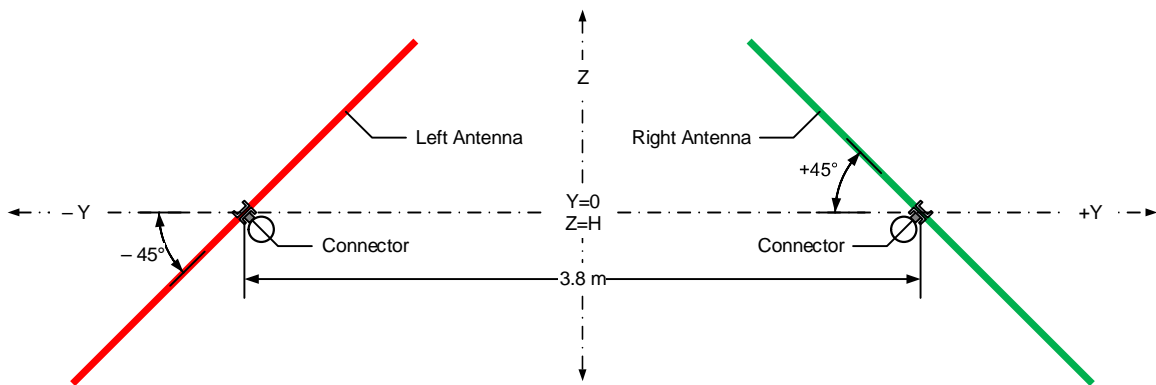


Figure 3 ~ Rear view drawing of crossed-dipole antennas showing perpendicular configuration and orientation with respect to horizontal. The axes are designated X, Y and Z for antenna modeling purposes. (Image © 2014, W. Reeve)

#### 4. Antenna Support Structure

In 2012 I built an antenna support boom structure from steel tubes and saddle clamps. However, the assembly weighed over 100 lb including the antennas. I did not look forward to placing it on the tower so discarded that idea and built another boom structure from aluminum tube as described in this section.

**Units of measure** ~ As stated in Parts 2 and 3, I seldom use non-metric units of measure in my articles but this series is an exception. As in previous parts, to help readers familiar only with metric units, I have provided a conversion table and a weblink to an online units converter in **section 13**.

The antenna support boom consists of a center hub section and two antenna mounts (figure 4). The center hub has telescoping sections to add strength to the boom. It attaches to the rotator and is moved in azimuth and elevation. The mounts separate the two antennas and extend them away from the center section. These mounts extend out from the boom 48 in to the front and 24 in to the rear. I provided the rear extensions in case I later decide to install antenna counter-weights. The structure uses a combination of bolted and welded components and weighs about 40 lb including antennas. The structure is such that the two antennas are separated by 3.8 m, and it may be modified in the future by replacing the bolted components.

The boom and mounts are 6061-T6 aluminum tube with 0.120 in wall thickness. The wall thickness provides a nominal 0.005 in clearance between the inside and outside diameters of the telescoping sections, which is just enough to ensure a smooth fit after considering manufacturing tolerances. All fasteners are 1/4-20 stainless steel (18-8). The inside diameter of the horizontal sleeve on the rotator limits the size of tube that may be used to 2 in, so that is the size of outer doubler over the support boom section tubes. I also used a 72 in long, 1.5 in outside diameter inner tripler for added strength. The outside diameter of the support boom sections is 1.75 in.

If permanently assembled the structure would be difficult to transport, erect and modify in the future. Therefore, I decided to use bolted flanges to hold each antenna mount to its associated center section boom tube. I precut and shaped all pieces in my own shop and then had a local machine shop do the welding (figure 5). The six welds required about 30 minutes each including setup. The antennas mount on the booms with saddle clamps (figure 6).

The distance between the antennas is about 1/3 more than the free space wavelength at 105 MHz (the low frequency design limit of the CLP5130-2N). I modeled this configuration using EZNEC antenna simulation software tool and will describe the results in a separate article.

An alternative boom structure configuration points the antenna longitudinal axes inward toward each other rather than parallel as described above. The angle would set to provide an equal number of wavelengths spacing from the low frequency end of the antenna to the high frequency end. This might be useful in an interferometer application; however, I am not interested in that type of observing for the application described in this article.

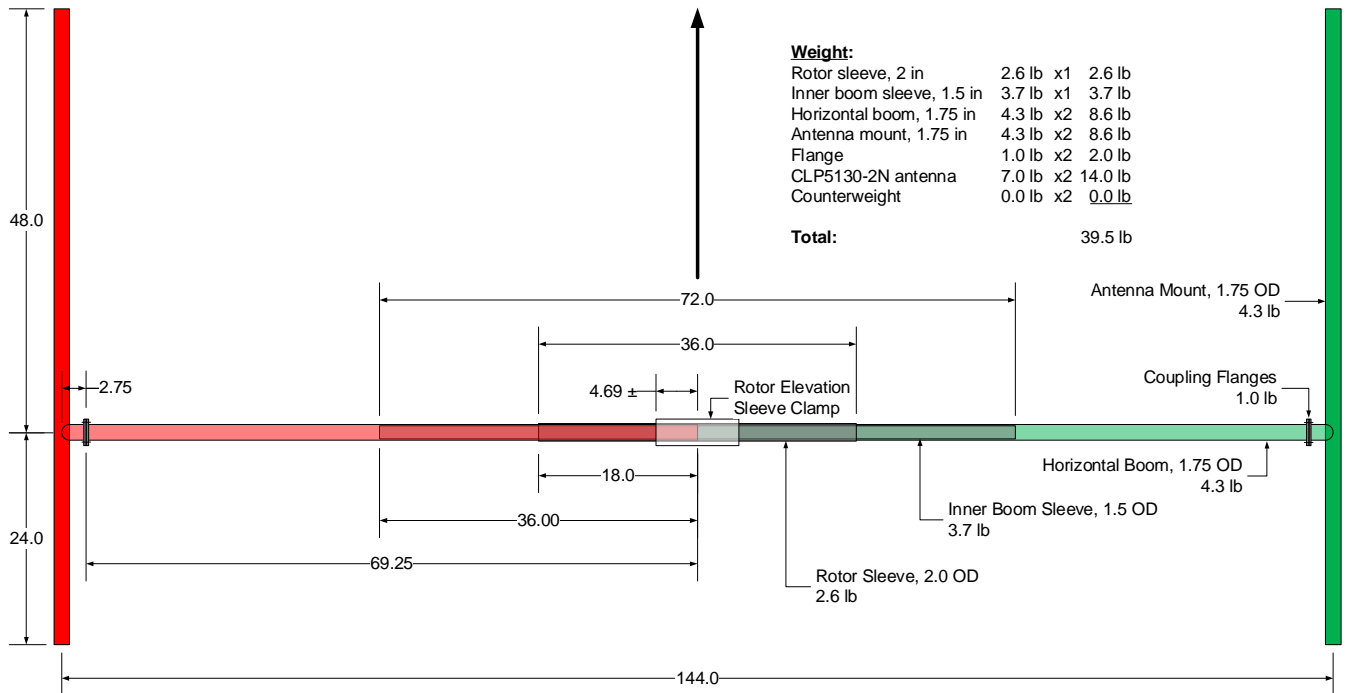


Figure 4 ~ Antenna support boom drawing as seen from above (dimensions in inches). The center section consists of three telescoping tubes with outside diameters of 2 in, 1.75 in and 1.5 in. The antennas (not shown) are installed on the antenna mounts on each side and top of the drawing. (Image © 2014, W. Reeve)



Figure 5 ~ Welds of the horizontal boom, antenna mount and flanges. The bolted flanges allow relatively easy field modifications to the antenna configuration. (Image © 2014, W. Reeve)



Figure 6 ~ One of two aluminum saddle clamps and stainless steel U-bolts supplied with each antenna for mounting on the antenna boom structure. The clamps are fastened to the bottom of the antenna's transmission line boom structure seen crossing the image diagonally bottom-left to top-right. (Image © 2014, W. Reeve)

## 5. Antenna Rotator

At my Anchorage observatory I use three Yaesu G-series rotators, two of which are used for daily Sun tracking. One tracking rotator was installed in 2008 and the other in 2011. These rotators use spur gears for rotation and a potentiometer for position feedback. I expected either the gear mechanism or pot to wear out in the oldest tracking rotator but did not know which would be first. It turned out the pot failed first. The problem revealed itself as occasional failure of the rotator controller to determine which direction to turn the antenna for parking after sunset; upon failure it turned in the wrong direction. The failure occurred only when the antenna was pointed in a certain direction at sunset but got worse with the season as the sunset azimuth changed and the potentiometer wiper moved through the worn out section. I finally was able to catch the failure and realize what the problem was but it actually took a couple years to nail it down. This rotator had been in daily Sun-tracking service for about five years.

For the Coho Radio Observatory, I looked at many different types and brands of rotators and finally chose the SPID Elektronik model RAS {[SPID](#)} (figure 7). The RAS uses a magnetically controlled reed switch in a pulse-counting circuit for position feedback. I believe this rotator originally was designed for satellite dish antenna applications. It uses worm gears rather than the straight spur gears used in the Yaesu and most other antenna rotators for amateur radio applications. The worm gear arrangement in the RAS produces smaller mechanical impulses when it is commanded to start and stop, thus reducing wear-and-tear compared to a rotator with spur gears. Also, unlike conventional rotators, the azimuth gear arrangement in the RAS has no rotation limit. This allows some flexibility when mechanically aligning the antennas with a reference direction (for example, true north as in the case of both my observatories) but the rotator control cables and antenna transmission lines ultimately limit the amount of rotation.



Figure 7 ~ SPID Elektronik model RAS azimuth-elevation rotator. The azimuth motor is visible at middle-right and associated gear and position sensing switch cover is just below it. Except for the vertical main mounting sleeve at the bottom, the entire assembly rotates. The elevation motor is on the opposite side. The elevation gear cover, visible at back-right, encloses one end of the elevation shaft sleeve. The control cable termination compartment is on the front immediately below the elevation sleeve. Eight 10 mm stainless steel bolts clamp the antenna boom (not shown) to the elevation sleeve. The bottom mounting sleeve also has eight 10 mm bolts to secure the vertical pipe mast. The rotator assembly weighs about 31 lb and is approximately 14 in high x 10 in wide x 9 in deep. The manufacturer, SPID Elektronik, is located in Żyrardów, Poland. I purchased the unit from RF HamDesign in The Netherlands. (Image © 2014, W. Reeve)

The RAS rotator mounts on a pipe mast having 2.67 in maximum outside diameter. I used an adapter between the tower top plate and the short mast for the rotator (figure 8). For the mast I used a 2.75 in outside diameter aluminum tube with 0.120 in wall thickness and a 2.5 in outside diameter aluminum tube to mount the rotator and to act as a mast doubler for added strength. The outer and inner tubes are held together and the outer section is held to the mast adapter with 1/4-20 stainless steel fasteners.



Figure 8 ~ Antenna rotator support mast and mast adapter. The mast adapter at the bottom is steel and the mast is two telescoping sections of aluminum tube. The mast adapter is attached to the tower top plate with 3/8-16 galvanized steel fasteners. The rotator's bottom sleeve (painted black and seen at top of picture) uses eight 10 mm stainless steel fasteners. All other fasteners are 1/4-20 stainless steel. A coil of the two rotator control cables is seen at the bottom. It loops around to the rotator out of the picture. (Image © 2014, W. Reeve)

The rotator control cables must be spiral-wrapped around the mast to accommodate rotation. The cables will unwrap as the rotator rotates clockwise while tracking the Sun and then re-wrap as it returns counter-clockwise to starts a new day. One wrap is needed for 360° rotation but I installed two wraps to provide redundancy and

flexibility in rotator alignment with true north. I initially made the rotator mast 24 in long (as shown in the pile of parts at the beginning of this article) but found during initial rotation testing that the cables became tangled too easily. I tried various methods to eliminate tangling and ended up shortening the mast to 12 in and using cable support brackets and cable clamps where the cables enter the rotator cable termination compartment and where the cables rise above the tower top plate (figure 9).

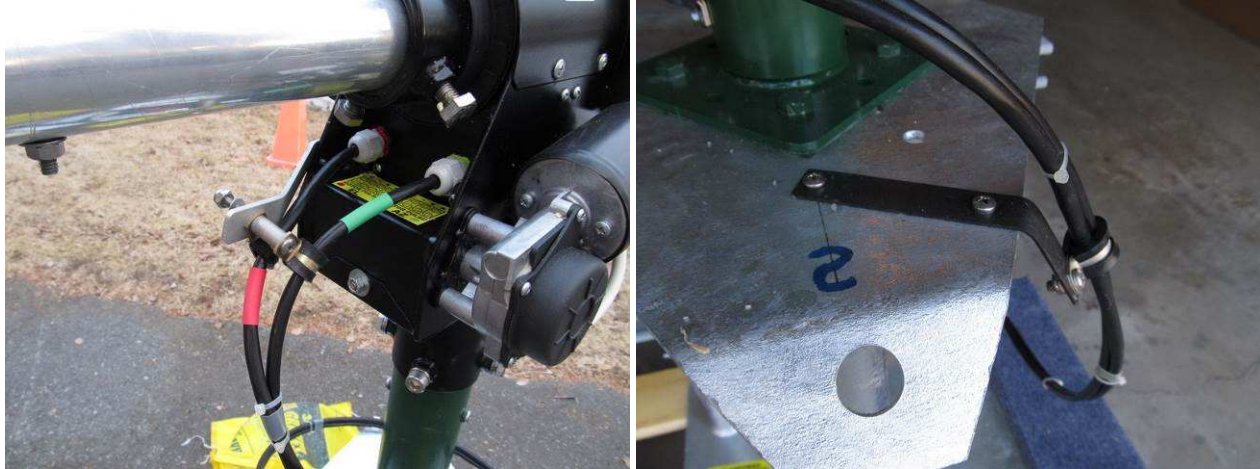


Figure 9 ~ Upper (left image) and lower (right image) rotator cable support brackets for strain relief. The cables are held to the brackets by Adel clamps. Cables enter the rotator terminal compartment through plastic strain relief bushings. (Image © 2014, W. Reeve)

The rotator control cables are 6-conductor, 18 AWG polyethylene insulated, 16/30 stranded, tinned copper in a polyethylene jacket (Wireman #311, {Wireman}). The rotator requires two conductors for each motor circuit and two conductors for each pulse-counting circuit, a total of eight conductors. To minimize voltage drop in the motor circuit, I decided to use one cable for each circuit combination (motor and pulse-counting circuit) and to use parallel conductors in the motor circuits, thus using all six conductors in each cable. The measured unloaded running current of each motor is approximately 1.4 A. The rotator uses dc motors so the current increases in approximate proportion to load. The information provided with the rotator indicates a normal load current of 2 to 3 A. I did some tests to determine the maximum stalled-rotator current on the motors and found it to be about 5 A.

The resistance of each control cable conductor  $R = 0.00715$  ohm/ft at 20 °C, so the loop resistance of the circuit would be  $2R$  (figure 10). When two conductors are paralleled, the resistance of each half of the loop circuit is  $R/2$ , and the loop resistance would be  $(R/2 + R/2) = R = 0.00715$  ohms/ft of circuit length.

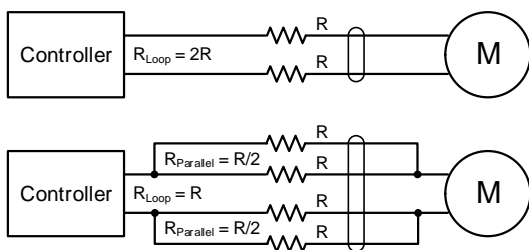


Figure 10 ~ Rotator motor circuit resistance with (bottom) and without paralleled conductors. (Image © 2014, W. Reeve)



Assuming a conservatively high total circuit length of 100 ft and a maximum load of 5 A, the voltage drop in the motor circuit will be

$$\text{Voltage drop at } 20\text{ }^{\circ}\text{C} = 5\text{ A} \times 100\text{ ft} \times 0.00715\text{ ohms/ft} = 3.6\text{ V}$$

It always is worthwhile to investigate the effects high ambient temperatures have on wire resistance and voltage drop. Cohoe is close to Alaska's Cook Inlet, a large body of glacier-fed river water mixed with ocean water from Gulf of Alaska. Historic weather records indicate temperatures seldom reach 30 °C. As a rule of thumb, the internal temperature of cables exposed to direct sunlight can rise 17 °C above ambient, in this case to 47 °C. This is 27 °C higher than the temperature used in the previous voltage drop calculation. The resistance of copper wire in ohms increases approximately 0.393%/°C; therefore,

$$\text{Voltage drop at } 47\text{ }^{\circ}\text{C} = 5\text{ A} \times 100\text{ ft} \times 0.00715\text{ ohms/ft} \times [1 + (0.00393/\text{ }^{\circ}\text{C} \times 27\text{ }^{\circ}\text{C})] = 4\text{ V (worst case)}$$

The normal operating voltage range of the SPID RAS motors is 12 to 24 Vdc. Operation below 10 V is not recommended. The speed of most dc motors is proportional to applied voltage. The azimuth rotation speed of the SPID RAS at 12 V is approximately 120 s/360°. To power the rotator, I will use a Meanwell SP-240-24 power supply rated 240 W, or 10 A at 24 V. It can be adjusted from 20 to 28 V. With its output set to 20 Vdc and 4 V worst-case voltage drop, the fully loaded motor voltage will be 16 V. The no-load voltage will be 20 Vdc, so both are well within normal operating range. Although the controller commands both azimuth and elevation simultaneously, the incremental rotations last less than 1 s while tracking the Sun.

The control cables from the rotator to the tower-mounted junction box are 10 ft long to accommodate two complete wraps around the mast and the drop into the junction box. The junction box is a NEMA 12 (gasketed rainproof) steel enclosure that I obtained surplus. I installed a terminal block inside (figure 11) to allow paralleling the motor circuit conductors in the cables running up the tower from the controller. The shorter cable from the junction box to the rotator does not use paralleled conductors. It was necessary to do it this way because the rotator terminal compartment would have been too crowded with a total of 12 conductors instead of 8 that are installed. I used dielectric grease on all connections in the rotator and junction box to reduce oxidation.



Figure 11 ~ Tower junction box with terminal block to enable termination and paralleling of the rotator control conductors. The box is 8 in high x 6 in wide x 4 in deep and has a rubber gasket on the hinged door. Ferrite beads for noise suppression are seen at bottom of enclosure. All cables are color coded to aid assembly and troubleshooting. (Image © 2014, W. Reeve)

The junction box is mounted just below the tower top plate on channel struts, and the struts are held to the tower legs with pipe clamps (figure 12). The junction box is large enough to accommodate clamshell ferrite beads on the circuits. I wrapped the wire from the J-box to the rotator three bifilar turns through the beads. Another junction box will be used at the receiver station to terminate the paralleled wires and for installation of an additional set of ferrite beads (figure 13).



Figure 12 ~ Front (left image) and rear view of channel struts for mounting the tower junction box and tower-mounted amplifier assembly. In the front view, the rotator cable junction box is seen mounted on left side. Holes for the tower-mounted amplifier enclosure are visible on right side. (Image © 2014, W. Reeve)

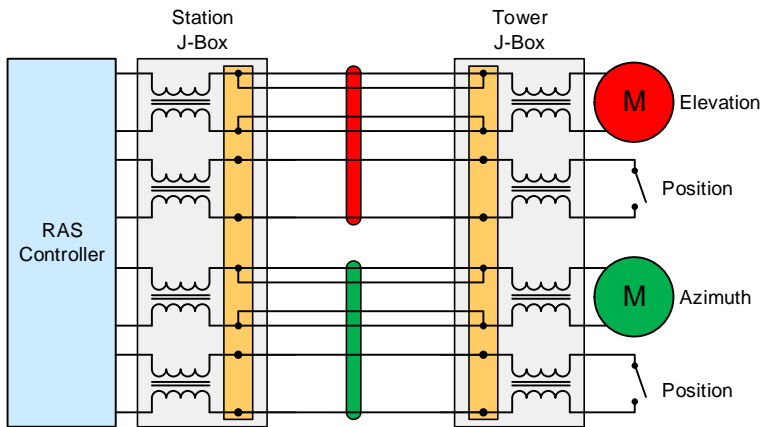


Figure 13 ~ Ferrite beads for noise suppression are installed at both ends of the rotator control cables. (Image © 2014, W. Reeve)

## 6. Rotator System Setup and Tests

After all components were fabricated, I assembled the rotator mast and plate adapter to the tower top plate and the rotator to the mast for preliminary testing indoors. I built test cables specifically for this purpose and setup the rotator controller (figure 14) as follows:

Control protocol: SPID  
 Azimuth and elevation rotation resolution: 1°

Normal azimuth rotation range:	0° to 359°
Allowable azimuth rotation range:	380° total, starting from 350° rotating clockwise through 180° to 10°
Physical azimuth rotation limits:	For rotator, none; For cabling, $360 \pm 180^\circ$
Normal elevation rotation range:	0° to 90°
Allowable elevation rotation range:	-5° to +90°
Physical elevation rotation limit:	0° to 180°

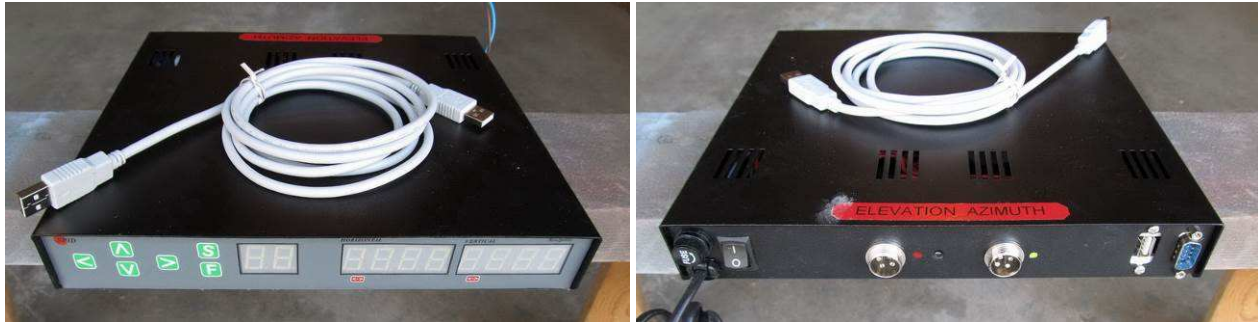


Figure 14 ~ Front (left image) and rear views of controller for RAS rotator. This unit uses 7-segment LEDs for azimuth and elevation displays. Controls for setup are tactile pushbutton switches covered with a membrane. The controller may be powered with up to 24 V ac or dc and uses circular connectors on the rear panel for the rotator cables. A specially modified mouse may be used for elevation and azimuth positioning through a DB9 connector on the rear panel. The controller connects to a PC through the USB port seen on the rear panel next to the DB9 connector at far right. (Image © 2014, W. Reeve)

The controller is put into the program mode and the parameter values are set using the arrow buttons on the control panel. After setup, the controller is put back into operating mode. It has three operating modes: Manual, Partial Automatic and Automatic. In Automatic mode, the controller receives solar tracking commands from a compatible software application. I use PstRotator software, which I will review in a future article. The controller receives commands and sends position data to a PC through the controller's USB port. For the initial tests I adjusted the PC time and date to around the summer solstice (21 June) to simulate maximum rotation in azimuth and elevation. I let the entire system run in my lab for about 2 weeks while I observed the cable wrapping at various times of the day. I also ran the rotator to its minimum and maximum limits using both manual and computer control.

All indoor tests were completed successfully in early March, and I was ready to move everything outdoors where I could assemble the antenna support structure, temporarily mount the two antennas, and run additional rotation tests. However, I decided to wait for warmer spring temperatures rather than try to troubleshoot any system problems in winter weather. Around the middle of April, the weather was pleasant enough to put everything together. I setup the tower top plate section on a spare tower base plate and held it down with a 50 lb lead weight (figure 15). I previously color-coded all components to speed reassembly and everything fit together perfectly as expected. I quickly aligned the antennas with respect to true north and then let the system run in Automatic mode for about 1 week. I found no problems so disassembled everything for transport to Coho later in the summer.



Figure 15 ~ Rotator test setup. The tower top plate is on a spare tower base plate held down with 50 lb lead weight on a furniture dolly (the two 60 lb bags of pea gravel prevent movement). The rotator mast adapter, rotator mast, rotator, junction box and rotator cables have been permanently installed, and the support booms and antennas are temporarily installed for testing. Red flags warn passerby's of the low visibility antennas. When this image was taken on 23 April 2014, the system was tracking the Sun, which was near transit (transit is when a celestial body crosses a north-south line about halfway between rising and setting). (Image © 2014, W. Reeve)

## 7. Tower-Mounted Amplifier Assembly

The model TMA-2 tower-mounted amplifier (figure 16) includes a bias-tee and a step-down linear voltage regulator. The TMA uses a NEMA 4X (watertight, corrosion resistant) polyester enclosure, which is completely sealed except for a small weep-hole at the bottom. It will be mounted with stainless steel fasteners on the channel struts previously described. The low noise amplifiers are Mini-Circuits ZX60-33LN+ [{MCL}](#) and each is equipped with a lightning arrester on its input. Only one of the two amplifier circuits from the LNA Power Coupler (LPC) carries dc, and that circuit has a limiter between the bias-tee and the amplifier. The limiter reduces the voltage spike coupled into the amplifiers from the bias-tee RF port (see [ReeveRAP] for a detailed discussion of this problem).

The TMA obtains 8 Vdc powering voltage from the LPC located in the observatory, and this is stepped down to 3.3 V for the amplifiers. The step-down power supply in the TMA has a low-current LED to indicate power. The

LPC is equipped with an identical bias-tee for power feed. A block diagram shows the complete low noise preamplifier system (figure 17). The bias-tees and limiter introduce a slight imbalance in the transmission circuits, which may reduce performance of the quadrature coupler as previously mentioned. This will be investigated later in the summer. Depending on the results, it may be necessary to rework the transmission and dc feed circuits so they are identical in all respects.



Figure 16 ~ Model TMA-2 tower-mounted amplifier shown without weatherproof cover. The polyester enclosure is 8 in high x 6 in wide x 4 in deep and has a rubber gasket on the removable cover. This unit is equipped with two low noise amplifiers (middle-left), lightning arrestors (bottom-left), bias-tee (top) with voltage limiter (top-left), step-down linear power supply and a bonding/grounding stud for the conductive components and lightning arrestors. (Image © 2014, W. Reeve)

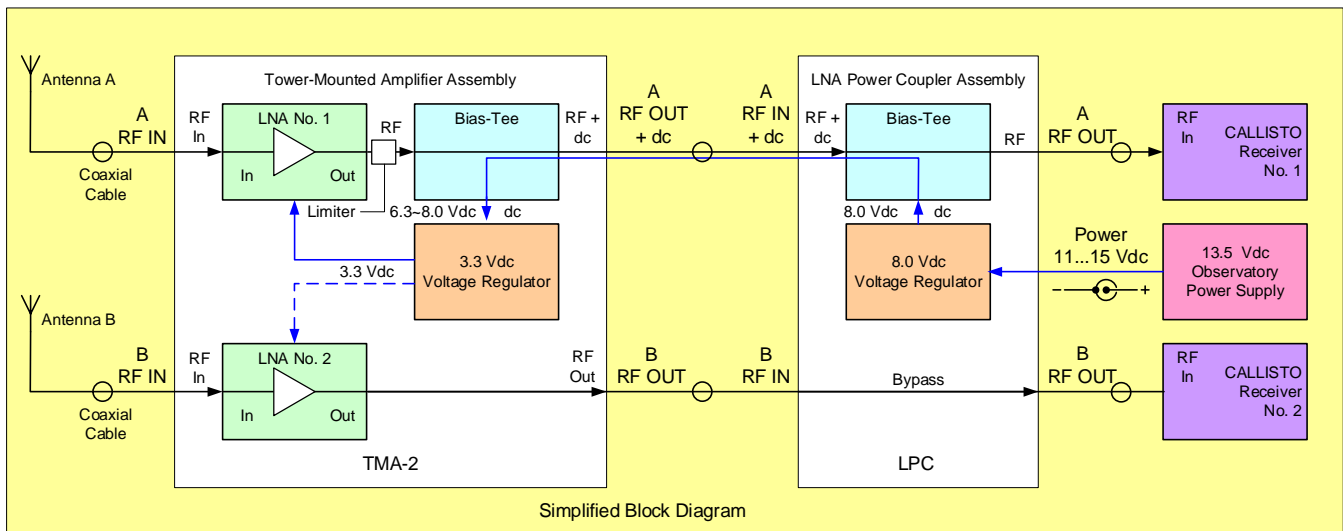


Figure 17 ~ Low noise amplifier system block diagram in a standard configuration consisting of the TMA-2 tower-mounted amplifier and LNA power coupler. The transmission balance between circuits A and B may need to be improved when this system is used with a quadrature coupler. In a standard configuration, only circuit A has bias-tees and a limiter and these have slightly different transmission loss and phase than circuit B. (Image © 2014, W. Reeve)

## 8. Transmission Line System

The transmission line system consists of coaxial cables from the antennas to the TMA and from the TMA to the observatory cable entrance. Only the antenna feedlines are described here. I faced the problem of wrapping a total of four cables around the rotator mast, two control cables and two coaxial cables. The cable route distance from each antenna to the TMA is 7.0 m, including 3.9 m from each antenna to the rotator and 3.1 m from the rotator to the TMA. To minimize transmission loss between the antenna and low noise amplifier, so that system noise figure is not degraded too much, I preferred to use Times Microwave LMR-400 cable for the entire distance. However, I felt that LMR-400 or LMR-400-UF (ultra-flexible) is too stiff so I decided to use LMR-400 from the antennas to the rotator and LMR-240-UF from the rotator to the TMA. LMR-400 is 10 mm diameter and LMR-240 is 6 mm diameter.

This arrangement is a compromise between stiffness and transmission loss. Each increment of transmission loss between the antenna and TMA degrades the system noise figure by an equal amount. Thus, an ideal installation would have the low noise amplifiers located at the antenna RF connector, but this is a mechanical impossibility. However, in my design – with the antennas on boom structures separated by 3.8 m and a standard tower-mounted amplifier assembly – I have to feed some distance as mentioned previously. If I had used LMR-400 for the entire distance, the degradation would be 1.0 dB at 900 MHz. The degradation would be 2.0 dB for LMR-240-UF. Using a combination gives 1.5 dB, a sacrifice of 0.5 dB in noise figure compared to using only LMR-400. Not to be forgotten are the slightly higher costs of the extra connectors. It should be noted that connector losses at 900 MHz and lower are negligible if they are good quality and properly installed.

I used right-angle male RF connectors at the antenna (figure 18), and a male-female connector combination at the interface between the LMR-400 and LMR-240-UF cables. The mating connector for the TMA is male. All connectors are crimp type N and will be sealed with self-fusing, conformable rubber mastic tape.



Figure 18 ~ Antenna RF connector (left) and associated right-angle type N cable connector. LMR-400 coaxial cable is shown adjacent to the antenna RF connector prior to connection and routing (the antenna is shown upside down; the connector is pointed downward in actual installation). The antennas will be mounted on their respective booms and RF connections made and sealed prior to raising the boom structure to the tower top. (Image © 2014, W. Reeve)

## 9. Costs (USD)

Log periodic antenna (2)	\$750
Rotator	\$1300
Aluminum tubing	\$100

Fasteners and hardware	\$50
Welding	\$335
Coaxial and control cable and connectors	\$100
Shipping and delivery	\$200
Fabrication and testing labor, 100 hours	<u>\$0</u>
Total	\$2835

## 10. Cohoe, Alaska

CRO is located in a rural area about 1 km southwest of where the Kasilof River flows into Cook Inlet and about 125 km southwest of Anchorage (figure 19). Coordinates for the site are 60° 22' 4.93"N, 151° 18' 55.76"W and elevation is approximately 21 m above mean sea level (AMSL). The site is near the old town of Cohoe. The observatory location came perilously close to destruction by a wildfire in May 2014 (figure 20).



Figure 19 ~ Aerial imagery of Alaska's Cook Inlet from 180 km altitude showing CRO (below-left of center). The outlet of glacier-fed Tustumena Lake (lower-middle) into the Kasilof River is about 16 km southeast of CRO. (Image courtesy of Google earth).

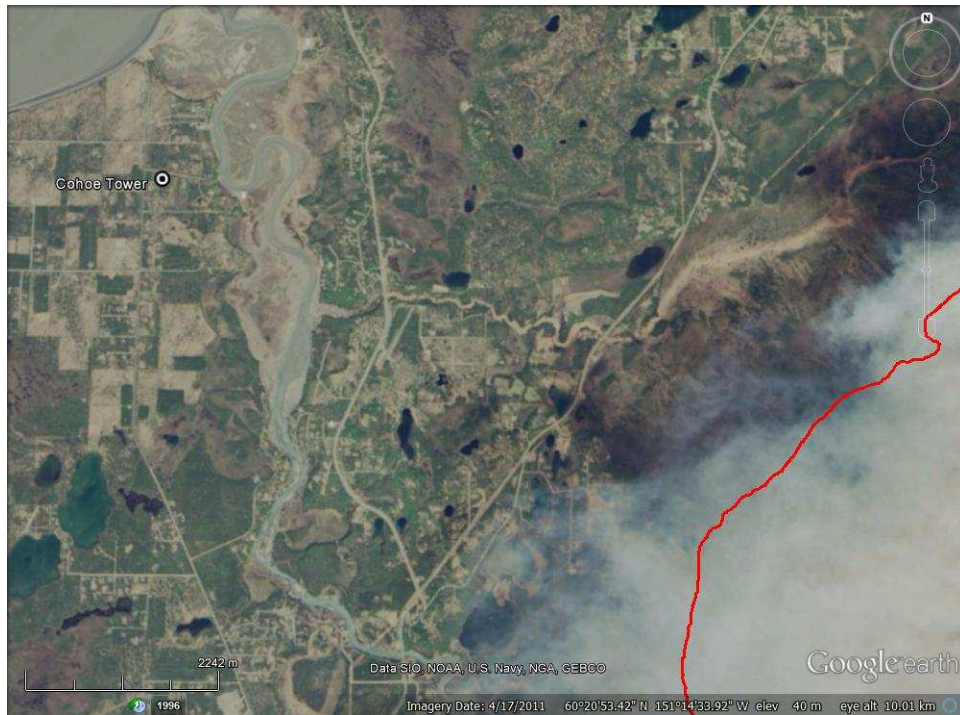


Figure 20 ~ Aerial imagery from 10 km altitude showing Cohoe Observatory location (small circle upper-left) and red wildfire line seen in lower-right corner as of 29 May 2014. The Sterling Highway cuts diagonally across the image from upper-right to lower-left. If the fire had crossed the highway, it needed to travel only 3 or 4 miles to Cohoe. Incredibly, the **193 000 acre** fire destroyed only five structures, an outbuilding and four recreational cabins, owing mostly to the remoteness of the area and sparse population, the efforts of 760 firefighters and smoke-jumpers including numerous water-bombing aircraft and helicopters, and finally some rain. The fire burned out of control for nine days and was manmade (accidental or intentional is not known). It was driven by wind and fed by extremely dry vegetation. (Image courtesy of Google earth).

## 11. Next step

The antenna system described here will be raised to the tower top during summer or fall 2014 after completion of the observatory itself. The observatory will be a wood-frame structure 24 ft long x 12 ft wide placed on a helical metal pile foundation. Site preparation and building construction, which is underway as this article is being written in May 2014, will be described in the next article in this series.

## 12. References and Web Links:

- [Reeve1] Reeve, W., Radio Frequency Interference Survey at Cohoe Radio Observatory, Alaska, *Radio Astronomy*, Society of Amateur Radio Astronomers, September-October 2013
- [Reeve2] Reeve, W., Cohoe Radio Observatory, Alaska ~ Part 2, Guyed Tower Foundation Construction, *Radio Astronomy*, Society of Amateur Radio Astronomers, November-December 2013
- [Reeve3] Reeve, W., Cohoe Radio Observatory, Alaska ~ Part 3, Guyed Tower Installation, *Radio Astronomy*, Society of Amateur Radio Astronomers, January-February 2014



[ReeveRAP] Reeve, W., Application Note on Remote Amplifier Powering, *Radio Astronomy*, Society of Amateur Radio Astronomers, January-February 2013

{e-Callisto} <http://www.e-callisto.org/>

{MCL} <http://www.minicircuits.com/homepage/homepage.html>

{ReevePol} [http://www.reeve.com/Documents/Articles%20Papers/Reeve\\_Polarization.pdf](http://www.reeve.com/Documents/Articles%20Papers/Reeve_Polarization.pdf)

{ReeveQC} [http://www.reeve.com/Documents/Articles%20Papers/Reeve\\_QuadCouplerApp.pdf](http://www.reeve.com/Documents/Articles%20Papers/Reeve_QuadCouplerApp.pdf)

{SPID} <http://www.spid.alpha.pl/english/11.php>

{TMA} <http://www.reeve.com/Solar/e-CALLISTO/e-callistoTMA.htm>

{Wireman} <https://www.thewireman.com/>

### 13. Units of measure conversion

Many unit converters can be found online: <http://www.digitaldutch.com/unitconverter/volume.htm>, but for convenience conversions of the non-metric units used in this article are shown below.

Convert from	To	Multiply by
acre	square kilometer (km <sup>2</sup> )	0.004
inches (in)	millimeter (mm)	25.4
feet (ft)	meter (m)	0.305
mile (mi)	kilometer (km)	1.6
pound (lb)	kilogram (kg)	0.454

## Document Information

Author: Whitham D. Reeve

Copyright: ©2014 W. Reeve

Revisions: 0.0 (Original draft started, 12 Feb 2014)  
0.1 (Edits, 14 Feb 2014)  
0.2 Continue work on 1<sup>st</sup> draft, 25 Apr 2014)  
0.3 (Add'l work on 1<sup>st</sup> draft, 2 May 2014)  
0.4 (Add'l work on 1<sup>st</sup> draft, 18 May 2014)  
0.5 (1<sup>st</sup> draft completed, 29 May 2014)  
1.0 (Final edits and distribution, 4 Jun 2014)  
1.1 (Added polarization and quadrature coupler references, 5 Jun 2014)

Word count: 5532

File size (bytes): 4192256